



NONO Regulates Cortical Neuronal Migration and Postnatal Neuronal Maturation

Xiaoqing Liu^{1,2} · Jiangli Zheng^{2,3} · Shaojun Qi^{2,3} · Qin Shen²

Received: 8 April 2019 / Accepted: 17 June 2019 / Published online: 9 September 2019
© Shanghai Institutes for Biological Sciences, CAS 2019

Dear Editor,

The mammalian cerebral cortex, responsible for all higher-order brain functions, is organized into six layers of neurons that form distinct projections and connections within and outside the cortex. During cortical development, neural progenitor cells (NPCs) in the proliferative ventricular zone (VZ) and subventricular zone (SVZ) of the dorsal telencephalon produce projection neurons that migrate toward the pial surface to form the cortical plate (CP). New-born neurons adopt a multipolar morphology with dynamic morphological rearrangement within the SVZ and the lower intermediate zone (IZ). This multipolar stage ends when cells extend a dominant pia-directed leading process and transform to a characteristic bipolar morphology [1–3]. This process is known as the multipolar-to-bipolar transition. After migrating radially to their correct position in the CP, neurons further develop a dendritic arborization, the basis of synaptic connections [4, 5]. Disturbance of neuronal migration can lead to severe

developmental defects and cortical malformations, which in turn cause neurological disorders such as schizophrenia, autism, and intellectual disability [6]. Although numerous genes have been implicated in cortical neuronal migration, the molecular mechanisms underlying this process are not yet completely understood.

We previously found that neural stem cells (NSCs) exhibit enhanced self-renewal when co-cultured with vascular endothelial cells [7]. One of the genes up-regulated in these NSCs is *Nono* (non-POU domain-containing, octamer binding protein) (data not shown). NONO, a nuclear DNA and RNA-binding protein, is involved in a variety of biological processes such as transcriptional regulation, RNA splicing, DNA repair, and tumorigenesis [8]. However, the spatiotemporal expression pattern and the role of NONO during embryonic cortical development are still unclear.

To elucidate the role of NONO in the developing mouse cortex, we immunostained for NONO in embryonic cortical sections from E11.5 to E17.5. At E11.5, when the cortical primordium only consists of the VZ and the pre-plate, we detected NONO in almost the whole cortex. The expression of NONO became higher in the CP and the VZ/SVZ but was relatively weak in the IZ from E13.5 to E17.5 (Fig. 1A). The mRNA expression pattern of *Nono* revealed by *in situ* hybridization at different stages was consistent with the protein expression obtained by immunostaining (Fig. S1A). Furthermore, the majority of p-Vimentin+ NPCs and Tuj1+ immature neurons were positive for NONO (Fig. 1B, C). NONO was expressed in most of the deeper-layer (Ctip2+ or Tbr1+) and upper-layer neurons (Satb2+ or Cux1+) (Fig. S1B, C). In contrast, <10% of cortical Tbr2+ intermediate progenitor cells were NONO+ (Fig. 1B, C), suggesting that the

Electronic supplementary material The online version of this article (<https://doi.org/10.1007/s12264-019-00428-y>) contains supplementary material, which is available to authorized users.

✉ Qin Shen
shenqin@tongji.edu.cn

- ¹ Peking-Tsinghua-NIBS Graduate Program, School of Life Sciences, Tsinghua University, Beijing 100084, China
- ² Tongji Hospital, Brain and Spinal Cord Innovative Research Center, School of Life Sciences and Technology, Frontier Science Research Center for Stem Cells, Ministry of Education, Tongji University, Shanghai 200092, China
- ³ Center for Stem Cell Biology and Regenerative Medicine, School of Medicine, IDG/McGovern Institute for Brain Research, Tsinghua University, Beijing 100084, China

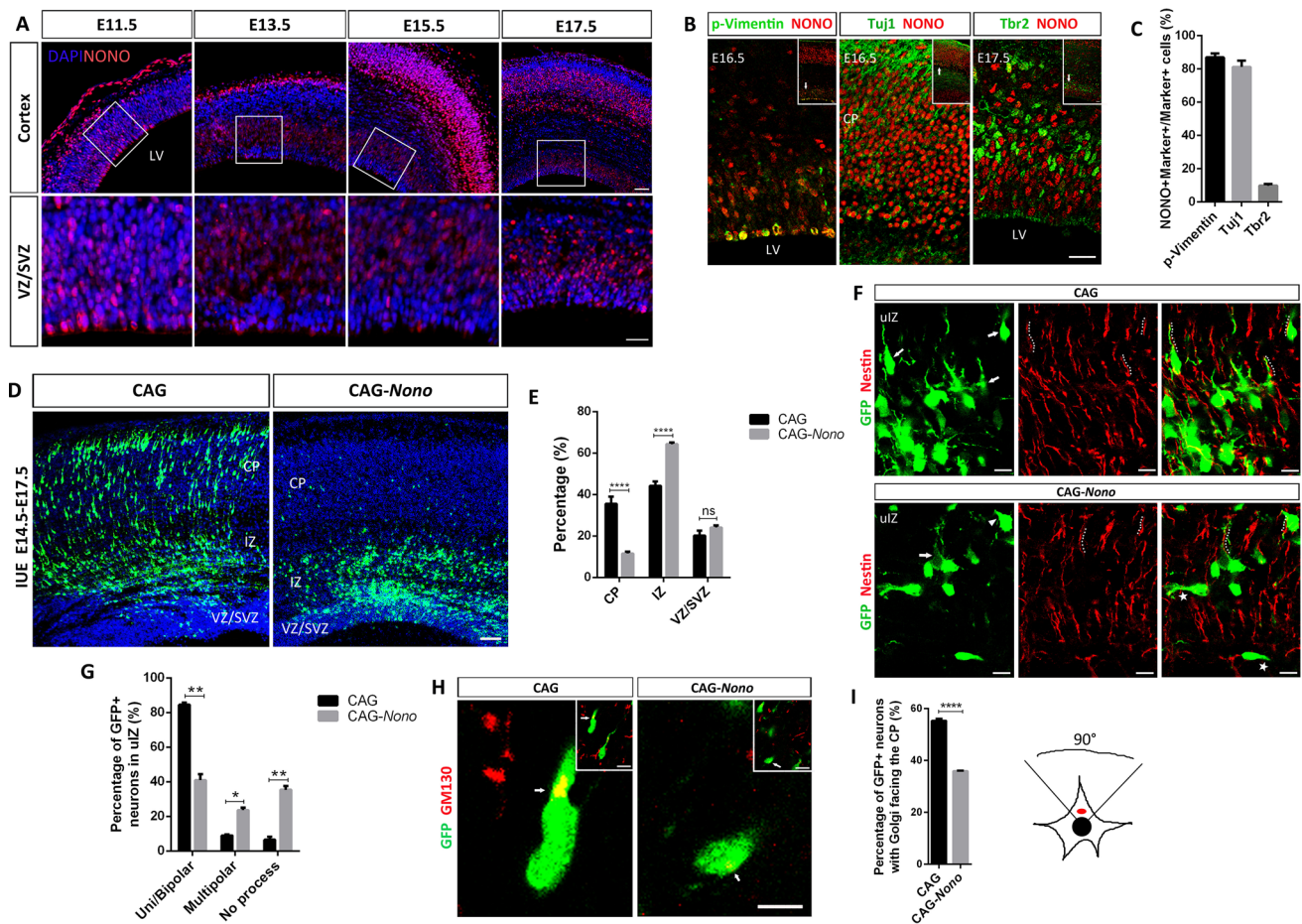


Fig. 1 NONO is expressed in the developing neocortex and regulates cortical neuronal migration. **A** NONO expression (red) in mouse neocortex from E11.5 to E17.5. Upper panels, low-magnification images of the cerebral cortex. Lower panels, high-magnification images of the boxed areas. Nuclei were counterstained with DAPI. LV, lateral ventricle (scale bars, upper, 50 μ m; lower, 25 μ m). **B** Co-staining of NONO (red) with p-Vimentin (green, left), Tuj1 (green, middle), or Tbr2 (green, right) in embryonic cortex (insets, low-magnification images). NONO was barely detected in Tbr2+ (green) cells (scale bar, 20 μ m). **C** Quantitative analysis of the percentages of NONO+ cells in different marker-expressing cell populations. Data represent the mean \pm SEM, $n = 3$ repeats, at least 80 cells were counted for each antibody in each experiment. **D** Fluorescence images of E17.5 cryosections from mouse embryonic cortex transfected with GFP-tagged *Nono* overexpression (right) or control (left) plasmids by *in utero* electroporation (IUE) at E14.5. VZ, ventricular zone; SVZ,

subventricular zone; IZ, intermediate zone; CP, cortical plate (scale bar, 50 μ m). **E** Quantitative analysis of images as in **D** showing the percentages of GFP+ cells in different cortical regions ($n = 6$). **F** Representative images showing the morphology of electroporated neurons in the upper IZ (uIZ) in E17.5 cortex. Radial glial fibers (dashed lines) were labeled with an anti-Nestin antibody (red). Arrows, uni/bipolar cells; asterisk/arrowheads, cells with abnormal leading processes (scale bars, 10 μ m). **G** Quantification of the percentages of GFP+ neurons with uni/bipolar, multipolar, or no process morphology in the upper IZ of E17.5 mouse cortex ($n = 4$). **H** Labeling of the Golgi apparatus with an anti-GM130 antibody (red, arrows) in CAG-GFP+ (left) and *Nono*-GFP+ cells (right) 3 days after IUE. Insets, low-magnification images (scale bars, 5 μ m; inset, 10 μ m). **I** Quantification of the percentages of GFP+ neurons with Golgi apparatus facing the CP in the IZ. The cartoon illustrates a multipolar neuron with the Golgi apparatus facing the CP ($n = 4$).

expression of NONO is regulated dynamically during the transition of NPCs to CP neurons.

We next electroporated GFP-expressing *Nono* shRNA or overexpression constructs (Fig. S2A) into the E14.5 mouse forebrain, and analyzed the distribution of GFP+ cells in the cortex at E17.5. There was a tendency for faster migration in *Nono*-shRNA neurons, as shown by a slight increase in the number of GFP+ cells in the CP and a decrease in the IZ, but the difference was not statistically significant (Fig. S2B, C). The result was similar with *in*

utero electroporation (IUE) at E12.5 (Fig. S2D, E). However, overexpression of *Nono* led to a dramatic decrease in GFP+ cells in the CP and an increase in the IZ (Fig. 1D, E). We also examined NPC proliferation and differentiation by immunostaining of Ki67 or co-electroporation of a pNeuroD1-mCherry construct, which drives mCherry expression in newborn cortical neurons [9] (Fig. S3A, C). We found that overexpression of *Nono* increased the percentage of Ki67+ cells ($24.2 \pm 0.3\%$ to $32.7 \pm 1.2\%$) and decreased the percentage of pNeuroD1-

mCherry+ cells ($31\% \pm 1.5\%$ to $23.1\% \pm 1.2\%$) (Fig. S3B, D). Taken together, these data suggest that NONO promotes NPC proliferation and inhibits differentiation and neuronal migration.

To investigate whether the failure of migration caused by *Nono* overexpression is due to a defective multipolar-to-bipolar transition, we analyzed the morphology of GFP+ neurons in the IZ. Most of the control GFP+ neurons were unipolar or bipolar and extended leading processes oriented toward the pial surface, often following along the long Nestin+ radial glial fibers (dashed lines in Fig. 1F). Overexpression of *Nono* significantly decreased the proportion of uni/bipolar neurons ($41\% \pm 3.5\%$ compared to $84.5\% \pm 1.2\%$ in control) and increased the proportion of multipolar neurons among all GFP+ cells in the upper IZ ($8.9\% \pm 0.6\%$ to $23.6\% \pm 1.4\%$) (Fig. 1F, G). The leading processes of *Nono*-overexpressing multipolar neurons appeared to be disoriented and deviated from the radial glial fibers (arrowhead in Fig. 1F), sometimes even with a horizontal leading process which was not associated with Nestin+ radial glial fibers (asterisk in Fig. 1F). These observations suggest that NONO regulates the multipolar-to-bipolar transition of cortical migrating neurons and their attachment to the radial glia.

The establishment of neuronal polarization is an important step during neuronal migration. When cells polarize, the Golgi apparatus is oriented toward the CP. We found that the Golgi apparatus, revealed by the Golgi matrix protein GM130, was oriented toward the CP in more than half of the GFP+ control cells ($55.3\% \pm 1.7\%$); however, following *Nono* overexpression, fewer GFP+ neurons showed correct Golgi apparatus orientation ($36\% \pm 0.6\%$, Fig. 1H, I). These data indicate that overexpression of *Nono* alters neuronal polarization.

NONO consists of two RNA recognition motifs (RRMs) and a NOPS (NONA/ParaSpeckle) domain [10]. We generated four GFP-NONO fragments that were truncated for the first RRM domain (nRRM1), the second RRM domain (nRRM2), both RRM (nRRM1+nRRM2), or the NOPS domain (nNOPS) (Fig. S4A, B), and electroporated them individually into the E14.5 mouse forebrain (Fig. S4C). We found that the distribution of GFP+ cells at E17.5 in the nNOPS group did not differ significantly from the control, and there were more GFP+ cells in the CP and fewer GFP+ cells in the VZ/SVZ in the nRRM1 group than in the control, opposite to the effect of *Nono* overexpression on neuronal migration. Interestingly, neuronal migration was markedly delayed in the nRRM2 group, which mimicked the effect of *Nono* overexpression (Fig. S4D). These results suggest that both the RRM1 and NOPS domains mediate the delay of migration, but RRM2 is not required.

We further performed IUE at E14.5 and analyzed the distribution of GFP+ cells at postnatal day 2 (P2), P7, P14, and P28. We confirmed that overexpression of *Nono* was persistently effective by staining for NONO in P28 brain sections (Fig. S6A, arrows). We divided the upper layers (marked by *Cux1*) into three equal parts and defined the rest of the cortex as the fourth part (Figs. S5A, S6B). Almost all of the GFP+ cells in the control group had reached the upper layer at P2, while $\sim 22\%$ of NONO-GFP+ cells were delayed in the region under the upper layer (Fig. S5A, B). We found that the migration delay was restored at P7 and later stages (Fig. S5C–F). In addition, there was a higher proportion of NONO-GFP+ cells in the more superficial upper layer than in the control (Fig. S5D, F), likely due to delayed differentiation and migration. The NONO-GFP+ cells left behind in the deeper layers at P2 expressed *Cux1* (Fig. S6B, arrows), supporting the notion of delayed migration rather than mis-specification of laminar fate.

Interestingly, we noted that the morphology of *Nono*-overexpressing GFP+ cells was different from the control cells at P7 and P28 (Fig. S5C, E). We analyzed the morphological differences of these neurons in detail at P14, a stage at which cortical migration is largely accomplished (Fig. 2A). We measured the length of the leading process, the number of primary processes, and the complexity of dendritic arborization in GFP+ neurons of control and *Nono* overexpression groups. *Nono* overexpression caused a dramatic loss of neuronal processes compared to control, with shorter leading processes, fewer primary processes, and less complex dendritic arborization (Fig. 2B–D). Three-dimensional imaging of P28 brain sections also showed that *Nono* overexpression led to remarkable morphological changes (Fig. S6C). Taken together, these data indicate that overexpression of *Nono* during NPC differentiation disrupts neuronal morphogenesis.

To further investigate the mechanisms that could account for the abnormal neuronal migration observed *in vivo* when *Nono* was overexpressed, we performed IUE at E14.5, and then sorted the GFP+ cells at E16.5 using fluorescence-activated cell sorting. We analyzed differentially-expressed genes (DEGs) between *Nono*-overexpressing cells and control cells using RNA-seq. Gene ontology analysis of DEGs that changed > 1.2 -fold revealed enrichment for neuron migration and neuron projection morphogenesis (Fig. 2E). Only 18 genes changed > 1.5 -fold when the *Nono* overexpression group was compared with the control (Table S1). One of these genes, vitronectin (*Vtn*), a secreted adhesive extracellular matrix glycoprotein mainly expressed in the meninges and capillaries of the embryonic cortex, is known to bind to integrin $\alpha v \beta 3$ and thus promotes cell adhesion and spreading [11, 12]. We confirmed that *Vtn* was induced in cortical cells by *Nono*

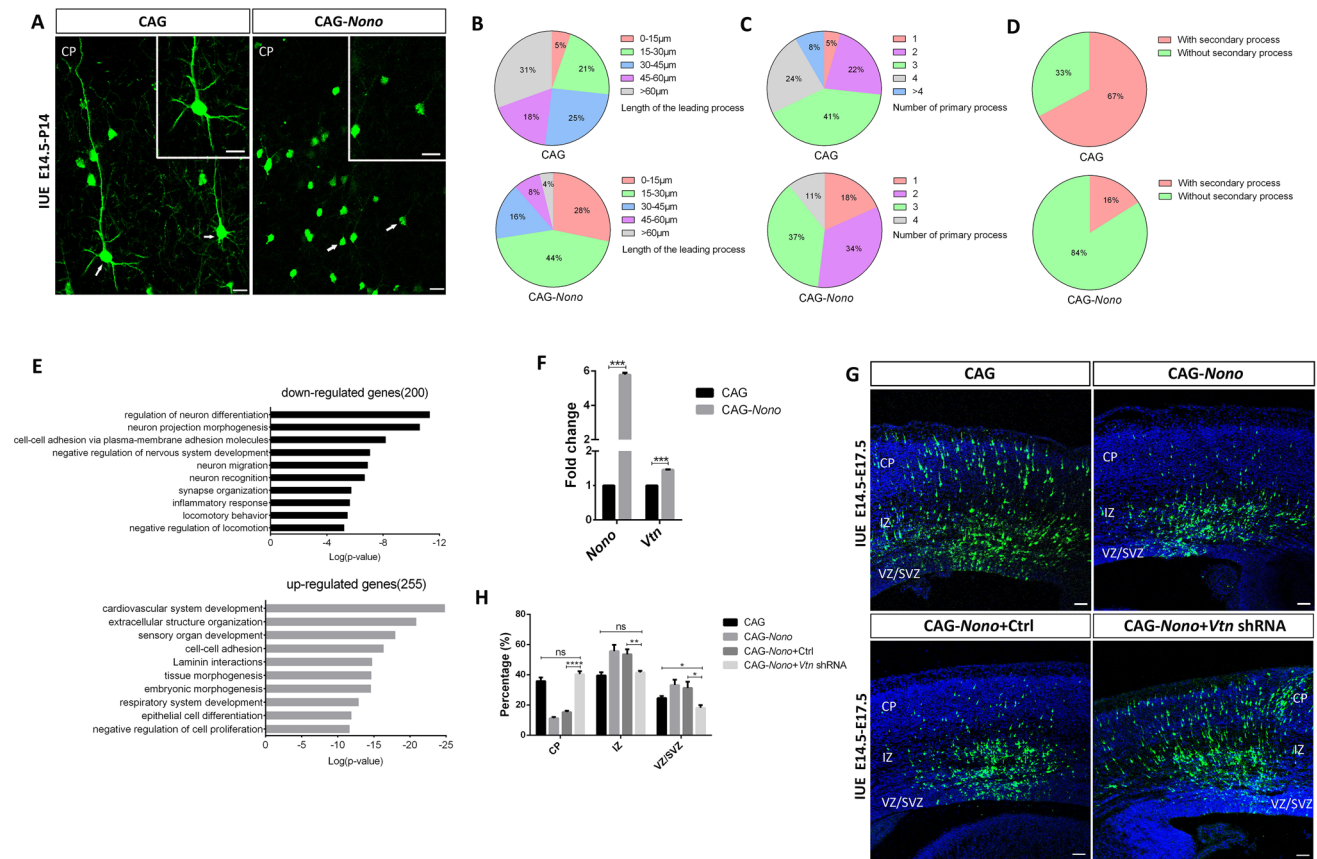


Fig. 2 NONO regulates postnatal neuronal morphogenesis and the expression of cell migration-related genes. **A** Representative images of cortical coronal sections showing the morphology of electroporated GFP⁺ neurons in the P14 cortical plate (insets, high-magnification images; arrows, transfected neurons). Scale bars, 20 μ m. **B–D** Quantitative analysis of GFP⁺ neurons such as those described in **A** ($n = 131$ cells for each) showing the length of leading processes (**B**), number of primary processes (**C**), and complexity of dendritic

arborization (**D**). **E** Gene ontology analysis of differentially-expressed genes differing by > 1.2 -fold between *Nono*-overexpressing and control neurons in E16.5 cortex. X-axis, $\log(p\text{-values})$. **F** qPCR analysis of vitronectin (*Vtn*) mRNA in *Nono*-overexpressing and control cells ($n = 3$). **G** Representative images of cortical coronal sections electroporated with the indicated plasmids at E14.5 and analyzed at E17.5 (scale bars, 50 μ m). **H** Quantification of the distribution of GFP⁺ cells as in **G** ($n = 3$).

overexpression using quantitative real-time PCR (Fig. 2F). Interestingly, there is an “ATGCAAAT” octamer NONO binding site 688 nt downstream of the *Vtn* mRNA sequence. Whether this functions as enhancer awaits further investigation. We found that forced expression of *Vtn* shRNA in *Nono*-overexpressing cells rescued the neuronal migration defects (Fig. 2G, H), indicating that *Vtn* is a candidate downstream target of NONO to regulate cortical neuronal migration.

The initiation of neuronal migration and the development of neurites are critical to the final positioning of neurons and the formation of neural circuits. Here, we demonstrated that disruption of the dynamic change of *Nono* expression by persistently overexpressing it from NPCs to neurons impaired the establishment of polarity in migrating neurons and the multipolar-to-bipolar transition, and consequently delayed neuronal migration and prevented the morphological maturation of neurons. Our

results indicate that transient downregulation of *Nono* in the IZ facilitates the transition of migrating neurons to the bipolar phase and is thus critical for their migration through the IZ. In our study, knock-down of *Nono* did not significantly affect the migration of cortical neurons. It is possible that knock-down of *Nono* was not sufficient and the remaining expression still fulfilled its function, as *Nono* is highly expressed in NPCs. Alternatively, other genes could compensate for the loss of *Nono* to ensure the proper development of the cerebral cortex. For example, SFPQ (splicing factor proline/glutamine rich) and PSPC1 (paraspeckle component 1) have functional redundancy with NONO, as all three are essential components of a nuclear domain called paraspeckle [8]. Previous studies have provided evidence that increased paraspeckle is directly associated with neurodegenerative diseases [13]. In human neuroblastoma tissue, a high level of *Nono* expression is correlated with a high level of N-Myc expression,

advanced disease stage, and a poor prognosis [14], implying that abnormally high *Nono* expression is relevant to disease. Taken together, our findings provide a novel understanding of the function of NONO in cortical development and have implications for neurodevelopmental disorders.

Acknowledgements We thank Dr. Frank Polleux (Columbia University, USA) for providing pNeuroD1-GFP plasmid and Dr. Yang Chen (Peking University, China) for sharing GM130 antibody. We are grateful to members of the Shen laboratory (Tongji University, China) for suggestions and comments. This work was supported by the National Natural Science Foundation of China (31371093 and 31671068), the Tsinghua Center for Life Sciences, and Tongji Hospital and School of Life Sciences and Technology, Tongji University, China.

Conflict of interest The authors declare that they have no conflict of interest in this work.

References

1. Tabata H, Nakajima K. Multipolar migration: the third mode of radial neuronal migration in the developing cerebral cortex. *J Neurosci* 2003, 23: 9996–10001.
2. Kriegstein AR, Noctor SC. Patterns of neuronal migration in the embryonic cortex. *Trends Neurosci* 2004, 27: 392–399.
3. Rakic P. Evolution of the neocortex: a perspective from developmental biology. *Nat Rev Neurosci* 2009, 10: 724–735.
4. Wang Y, Li WY, Li ZG, Guan LX, Deng LX. Transcriptional and epigenetic regulation in injury-mediated neuronal dendritic plasticity. *Neurosci Bull* 2017, 33:85–94.
5. Parrish JZ, Emoto K, Kim MD, Jan YN. Mechanisms that regulate establishment, maintenance, and remodeling of dendritic fields. *Annu Rev Neurosci* 2007, 30: 399–423.
6. Guerrini R, Parrini E. Neuronal migration disorders. *Neurobiol Dis* 2010, 38: 154–166.
7. Shen Q, Goderie SK, Jin L, Karanth N, Sun Y, Abramova N, *et al.* Endothelial cells stimulate self-renewal and expand neurogenesis of neural stem cells. *Science* 2004, 304: 1338–1340.
8. Shav-Tal Y, Zipori D. PSF and p54(nrb)/NonO—multi-functional nuclear proteins. *FEBS Lett* 2002, 531: 109–114.
9. Guerrier S, Coutinho-Budd J, Sassa T, Gresset A, Jordan NV, Chen K, *et al.* The F-BAR domain of srGAP2 induces membrane protrusions required for neuronal migration and morphogenesis. *Cell* 2009, 138: 990–1004.
10. Yang YS, Hanke JH, Carayannopoulos L, Craft CM, Capra JD, Tucker PW. NonO, a non-POU-domain-containing, octamer-binding protein, is the mammalian homolog of *Drosophila* nonAdiss. *Mol Cell Biol* 1993, 13: 5593–5603.
11. Seiffert D, Iruela-Arispe ML, Sage EH, Loskutoff DJ. Distribution of vitronectin mRNA during murine development. *Dev Dyn* 1995, 203: 71–79.
12. Zhou A, Huntington JA, Pannu NS, Carrell RW, Read RJ. How vitronectin binds PAI-1 to modulate fibrinolysis and cell migration. *Nat Struct Biol* 2003, 10: 541–544.
13. Nishimoto Y, Nakagawa S, Hirose T, Okano HJ, Takao M, Shibata S, *et al.* The long non-coding RNA nuclear-enriched abundant transcript 1_2 induces paraspeckle formation in the motor neuron during the early phase of amyotrophic lateral sclerosis. *Mol Brain* 2013, 6: 31.
14. Liu PY, Erriquez D, Marshall GM, Tee AE, Polly P, Wong M, *et al.* Effects of a novel long noncoding RNA, lncUSMycN, on N-Myc expression and neuroblastoma progression. *J Natl Cancer Inst* 2014, 106. pii: dju113.